Environmental Processes

Aerobic and Anaerobic Bacterial Mercury Uptake is Driven by Algal Organic Matter Composition and Molecular Weight

Vaughn Mangal, Benjamin Robert Stenzler, Alexandre J. Poulain, and Celine Gueguen

Environ. Sci. Technol., **Just Accepted Manuscript** • DOI: 10.1021/acs.est.8b04909 • Publication Date (Web): 05 Dec 2018

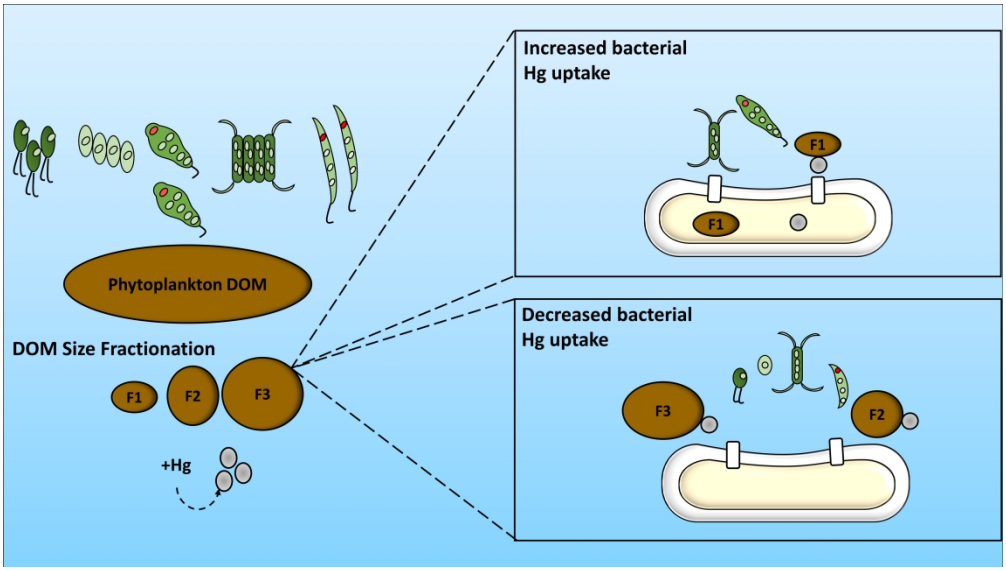

TOC Art

338x190mm (300 x 300 DPI)

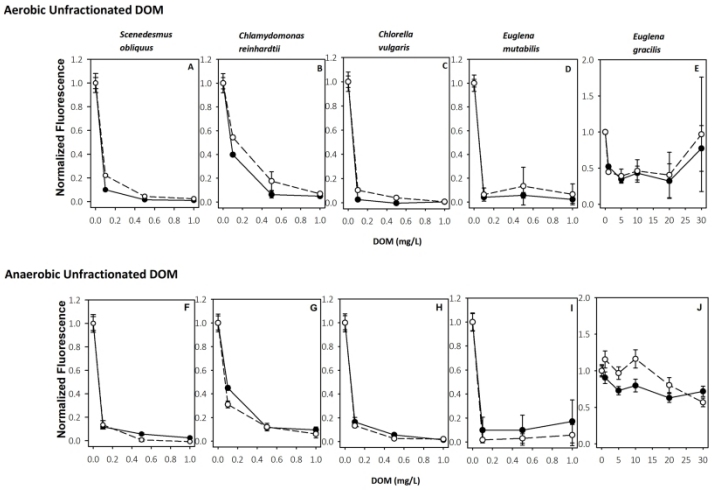

Figure #1: Aerobic (A-E) and anaerobic (F-J) bioassays with increasing DOM concentrations from algal cultures of S. obliquus (A, F), C. reinhardtii (B, G), C. vulgaris (C, H), E. mutabilis (D, I) and E. gracilis (E, J) where n=3.

338x190mm (300 x 300 DPI)

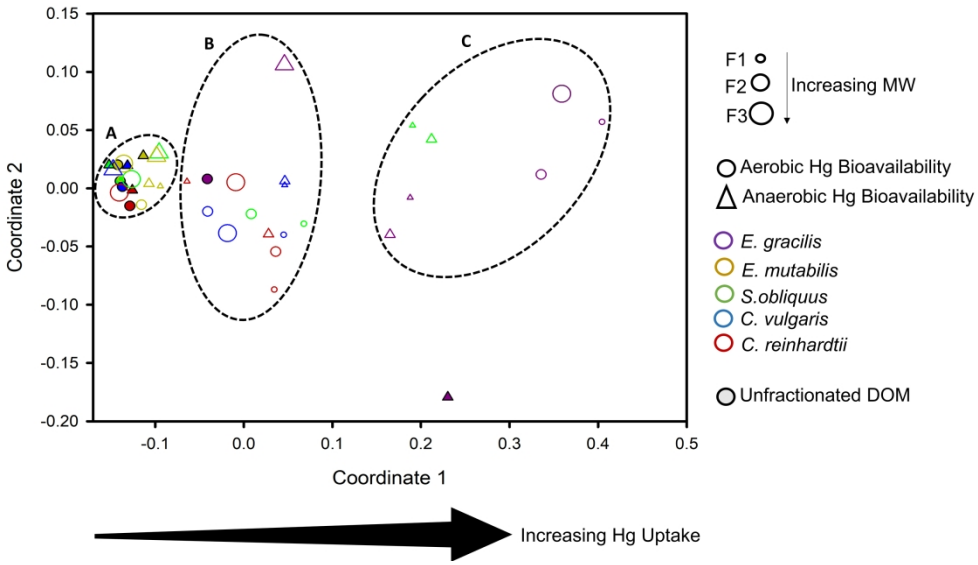

Figure #2: NMDS using a Euclidian measure analysis portraying the effect of algal DOM fractionation and Hg uptake. represent aerobic assays whereas represent anaerobic bioassays with the size of each symbol corresponding to the molecular weight fraction with =F1, =F2 and =F3. Colours correspond to algal taxa where purple is E. gracilis, yellow is E. mutabilis, green is S. obliquus, blue is C. vulgaris, and red is C. reinhardtii. Filled symbols outline unfractionated DOM and dashed lines show significant clustering.

338x190mm (300 x 300 DPI)

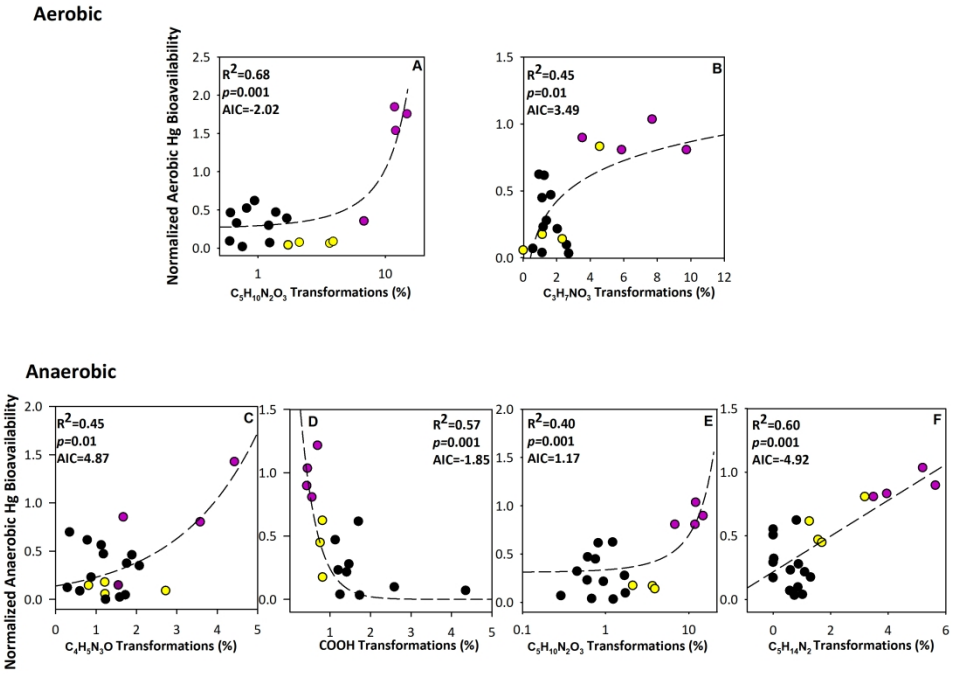

Figure #3: Significant Model II regression models outlining relationships between aerobic Hg uptake and C5H10N2O3 (glutamine; A), and C3H7NO3 (serine; B) isomers. Anaerobic Hg uptake and biomolecules are also expressed for C4H5N3O (cytosine; C), COOH functional groups (D), C5H10N2O3 (glutamine; E) and C5H14N2 (polyamine; F) isomers. Both Euglenoids are highlighted where yellow corresponds to points corresponding to E. mutabilis and purple highlights points influenced by E. gracilis.

296x209mm (300 x 300 DPI)

Aerobic and Anaerobic Bacterial Mercury Uptake is Driven by Algal Organic Matter Composition and Molecular Weight

Vaughn Mangal.[a$], Benjamin Stenzler,[b$], Alexandre J. Poulain.[b*], Celine Guéguen [c*].

[a] Environmental and Life Sciences Graduate program, Trent University, 1600 West Bank Drive Peterborough ON, Canada, K9J 7B8

[b] Biology Department, University of Ottawa, 30 Marie Curie, Ottawa ON, Canada, K1N 6N5

[c] Chemistry Department, Trent University, 1600 West Bank Drive Peterborough ON, Canada, K9J 7B8

[*] Corresponding authors: Alexandre J. Poulain & Celine Guéguen

[$] authors contributed equally to this work

Email addresses: apoulain@uottawa.ca; celinegueguen@trentu.ca

Telephone: 1-613-562-5800 ext. 2373; 1-705-748-1011 ext. 7859.

Abstract

The biological mobilization of mercury (Hg) into microbes capable of Hg methylation is one of the limiting steps in the formation of the neurotoxin methylmercury (MeHg). Although algal dissolved organic matter (DOM) has been associated with increased MeHg production, the relationship between bacterial Hg uptake and algal DOM remains unexplored. In this study, we aimed to address how the quantity and quality of DOM freshly harvested from several algae affected the bacterial uptake of Hg using a biosensor capable of functioning both aerobically and anaerobically. We combined biosensor measurements with high resolution mass spectrometry and field-flow fractionation to elucidate how DOM composition and molecular weight influence microbial Hg uptake. We showed that freshly harvested DOM from Chlorophyte and *Euglena mutabilis* strongly inhibited aerobic and anaerobic Hg uptake, whereas DOM harvested from *Euglena gracilis* did not exhibit this same pronounced effect. Once fractionated, we found that amino acids and polyamines, most abundant in *Euglena gracilis* DOM, were positively correlated to increase Hg uptake, suggesting that these molecules are potentially underappreciated ligands affecting Hg bioavailability. As water quality is affected by eutrophication, algal community assemblages will change, leading to variations in the nature of autochthonous DOM released in aquatic systems. Our results highlight that variations in the emergent properties of DOM originating from varying algal species can have a profound effect on bacterial Hg uptake and thus methylation.

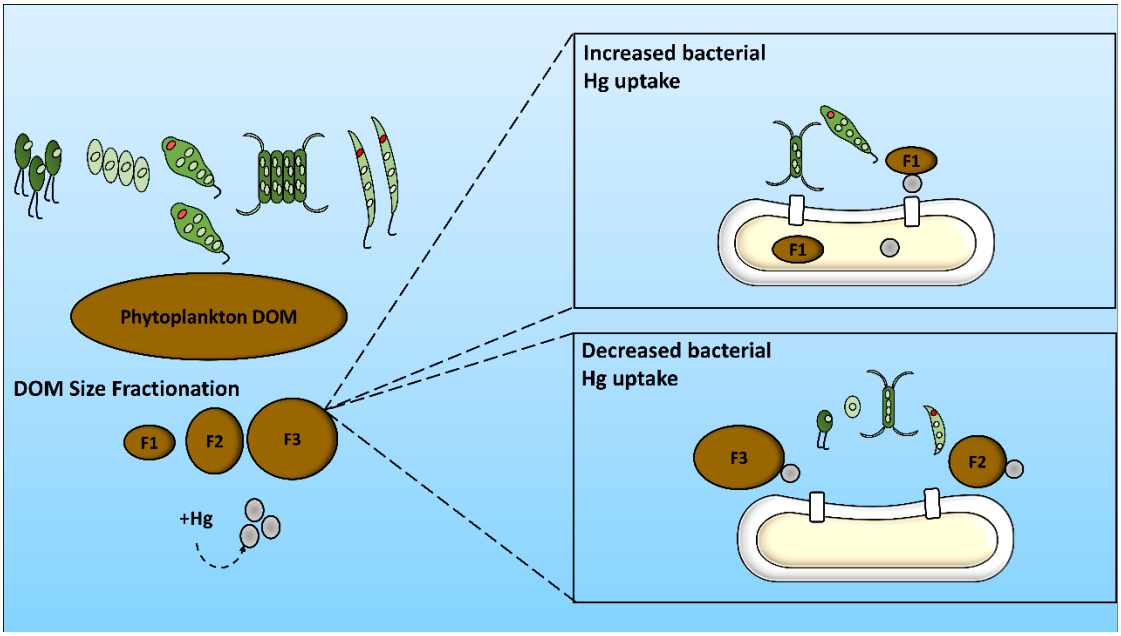

Introduction

Mercury (Hg) is a naturally occurring element and its mobilization through anthropogenic mining extractions and fossil fuel combustion has led to increased Hg and methylmercury (MeHg) concentrations in aquatic and terrestrial ecosystems. The biomagnification of MeHg in food webs can result in neurodegenerative disorders, ultimately affecting humans and wildlife[1-3]. Conversion of inorganic Hg to MeHg is predominately a microbially mediated process most notably performed by chemotrophic, anaerobic microbes[4]. Hg methylation is predicted to mostly occur in anoxic sediments, but alternative sites conducive to MeHg production have been identified in environments with enhanced photosynthetic activity and exhibiting dynamic redox interfaces such as chlorophyll maximum layers in polar marine waters[5-6], sea ice[7-8] or periphytic biofilms[9-11]. Because Hg methylation is thought to be an intracellular process[12], these recent discoveries emphasize the need to assess how phototrophic primary producers can impact microbial Hg uptake in oxic and hypoxic environments.

Studies investigating the role of primary producers on Hg methylation face the challenge of distinguishing their direct involvement as methylators from the indirect role they have in supplying nutrients to chemotrophic MeHg producers[13-15]. There is currently very little support, however, for phototrophs participating directly in Hg methylation[16]. It is most likely that primary producers affect Hg^{II} methylation by i) providing a substrate that affects the activity of Hg methylating microbes[17-19]; ii) releasing methylating compounds that would abiotically methylate Hg^{II} (e.*g.*, CH3Cl/Br/I or dimethylsulfoniopropionate)[20] and/or iii) releasing chemical ligands that can affect the uptake of Hg^{II} by methylators[11].

A necessary and rate limiting step in Hg methylation is the uptake of Hg to methylating microbes. Hg bioavailability is dependent on its chemical speciation, and in aquatic ecosystems, dissolved organic matter (DOM) is one of the most important metal binding ligands[21-22]. Hg bioavailability depends on DOM concentrations[23-25], molecular composition[26-28] and molecular weight[29]. More recently, studies have shown that DOM can also exert ecological controls on Hg methylation by affecting anaerobic microbial community structures[18-19]. DOM is heterogeneous, complex, and varies in concentration and composition across aquatic systems. Although allochthonous DOM transported to lakes can represent a significant proportion of the measured DOM in eutrophic freshwaters, microorganism-derived autochthonous DOM is typically more

labile, exhibiting rapid turnover rates that can significantly impact lake ecosystem functions[30]. On-going warming and changing aquatic nutrient loading from agricultural practices[31] affect algal assemblages in freshwater and marine systems, ultimately impacting the quality of DOM[32]. Furthermore, increased anthropogenic pressures on aquatic systems can lead to eutrophication[33], which can affect primary producer communities by selecting for more competitive and resilient species[34]. Due to inherent variability of DOM, characterization of DOM-Hg interactions is difficult[35-36]. Therefore, a multi-pronged analytical approach addressing not only DOM quantity and quality, but also accounting for Hg bioavailability is essential to support efforts required to predict and improve management of Hg pollution. A link between algal DOM and increased MeHg concentrations has been established[18-19, 27], yet we still do not understand the mechanisms by which this occurs. To address these missing links, our study focuses on the role that algal DOM has on microbial Hg uptake; one of the initial steps of Hg methylation.

In this study, we harvested and fractionated DOM produced by a diverse set of primary producers of the divisions Chlorophyta (*Scenedesmus obliquus, Chlorella vulgaris, Chlamydomonas reinhardtii)* and Euglenozoa *(Euglena gracilis* and *Euglena mutabilis).* These algal species are common in a diverse array of aquatic systems including biofilms associated high Hg methylation rates[11,37-38]. To understand how algal DOM impacts microbial Hg uptake, we used a unique combination of analytical techniques including asymmetrical flow field-flow fractionation (AF4) to separate DOM based on molecular weight[39-41] and high-resolution mass spectrometry (Fourier-transform ion cyclotron resonance mass spectrometry) to gather DOM compositional information[42], while assessing aerobic and anaerobic bacterial Hg uptake using a flavin-based whole cell biosensor[43]. Our study offers novel insights into the complexity of algal DOM and how it can affect the fate of Hg in aquatic ecosystems.

Materials and Methods

Algal Growth and Sample Preparation

We axenically cultured a total of five algal species including *Scenedesmus obliquus (S. obliquus), Chlorella vulgaris* (*C. vulgaris*), *Chlamydomonas reinhardtii* (*C. reinhardtii), Euglena gracilis* (*E. gracilis*) and *Euglena mutabilis* (*E. mutabilis*), obtained from the Canadian Phycological Culture Center (Waterloo, Canada). All algae were grown at 21°C at a 16:8 light/dark cycle. Bold basal medium (BBM) was used to culture *C. vulgaris* and *S. obliquus*, high

salt medium (HSM) for *C. reinhardtii,* and Hutner medium for both *E. gracilis* and *E. mutabilis* [39,44]. Once cultures were in mid exponential growth at 2.0 x 10^6 cells determined by cell hemocytometer counts, DOM was extracted by filtering through a 0.2µm Whatman filter. In addition to algal DOM, a Suwannee River Fluvic Acid (SRFA) standard obtained from the International Humic Substances Society (IHSS) was used for concentration and fractionation bioassays for comparison. Both SRFA and algal DOM were stored at 4°C in the dark for subsequent DOC analyses, fractionation and high-resolution mass spectrometry.

Asymmetrical Flow Field-Flow Fractionation (AF4) and DOC Analysis

To test for the role of the various size fractions of the DOM pool on Hg bioavailability, we performed a gentle separation of DOM based on molecular weight using asymmetrical flow field-flow fractionation (AF4)[41]. The AF2000 Focus fractionation system from Postnova Analytics coupled to a multichannel on-line spectrophotometer diode array detector (Shimadzu SPD-M20A) and fraction collector (Varian ProStar 701) equipped with a 300 Da polyether sulfonate (PES, Postnova Analytics) was used to separate and isolate DOM based on molecular weight[40]. The axial, focus, and cross flow settings were 0.25, 2.2 and 2.45 mL min^{-1}, respectively[39]. A calibration solution of macromolecular proteins was utilized to separate algal DOM and SRFA based on molecular weight. Two mL of a 5 mg-C L^{-1} of SRFA and algal DOM was injected into a 300µL sample loop. Fractions were collected during the elution step of fractionation at 1-minute intervals, over the course of 3 min, to acquire three distinct molecular weight groups using a fraction collector. Fraction 1 (F1) comprised of low molecular weight DOM (F1: 300-500 Da), fraction 2 (F2) consisted of medium molecular weight material (F2: 501-1000 Da) and the final third fraction comprised of the largest molecular weight material (F3: 1000-2000 Da) (Figure S1). Fractions were not collected below 300Da due to the membrane molecular weight cut off-of the AF4 and above 2000Da due to the low abundance of DOM. During fractionation, the eluent was adjusted by using ultrapure water, NaOH and HCl to modify pH, and a concentrated NaCl solution to match the conductivity of the injected algal DOM samples.

DOC concentrations were measured using a Shimadzu total organic carbon analyzer (TOC-V_{CPH}) (Figure S2). Calibration curves were run with a minimum of 5 concentrations standard (prepared gravimetrically) of potassium hydrogen phthalate in ultra-pure UV-oxidized water.

Aerobic and Anaerobic Bioassays

Both aerobic and anaerobic bioassays were conducted as per Stenzler et al. (2017)[43]. Two *Escherichia coli* biosensors were used; one was a Hg inducible biosensor (*E. coli* NEB5α harboring the pUC57merR-Pp plasmid) where the production of a flavin based fluorescent protein (FbFP) was under the control of *merR* [the transcription regulator of the *mer* operon]. The other was a constitutive biosensor (*E. coli* NEB5α harboring the pUC19AH206-Pp plasmid), which expressed the FbFP irrespective of the presence of Hg. Experiments with both biosensors were performed in parallel to control for the effect of the conditions tested on cell health. From a -80˚C cryostock, cells were grown and selected for on lysogeny broth (LB) agar plates exposed to 210µg mL^{-1} ampicillin and grown at 37˚C. Colonies were selected from the plate and grown in LB before transferred (an)aerobically in the growth medium described in Stenzler et al. (2017)[43]. Growth was monitored until an optical density at 600 nm (OD_{600}) of 0.6 was reached. Cell growth was subsequently halted by resuspending in the (an)aerobic BMAA exposure medium to be used as a cell stock in the following bioassay.

All pipetting and exposures were conducted in an anaerobic chamber (97% $N_{2\,(g)}$ and 3-4% $H_{2\,(g)}$). Assays were mixed in a 7mL Teflon vial, along with BMAA exposure medium, and either unfractionated DOM at increasing concentrations for bulk assays, or AF4 fractions normalized to 1mg L^{-1} carbon for molecular weight assays in both aerobic and anaerobic settings. Hg was diluted from an 8 µmol L^{-1} stock solution of $HgSO_4$ to a final concentration of 5nmol L^{-1} in the Teflon vials to equilibrate with the DOM. After equilibrating, aerobic samples were removed from the anaerobic chamber, and aerated under a sterile field. Both aerobically or anaerobically, 100µL of the cell stock was added to the Teflon vials and immediately transferred to a 96 well plate to be measured at 37°C on a Tecan Infinite Pro plate reader at fluorescence 450 ± 10 nm and emission wavelengths of 500 ± 20nm for aerobic assays. Anaerobic fluorescence was measured in the anaerobic chamber on a Synergy HTX plate reader at fluorescence excitation of 440/40 mm and emission fluorescence at 500/27 nm. Analytical triplicates were conducted on plate readers and biological duplicates were considered for both aerobic and anaerobic assays. A constitutive bacterial strain was also grown that emits fluorescence irrespective of the presence of Hg[45], and exposed to comparable DOM concentrations and fractions to explore the role of DOM on *E.coli's* ability to emit fluorescence. These values were

normalized to the inducible strain results. To compare biological replicates, bioassay results were also normalized to the 5 nmol L^{-1} control fluorescence.

Fourier Transform Ion Cyclotron Mass Spectrometry

A 7T Bruker SolariX XR Fourier Transform Ion Cyclotron Resonance Mass Spectrometer (FT ICR MS) (Billerica, Massachusetts) equipped with an electrospray ionization (ESI) source and a ParaCell ICR cell was used to characterize DOM composition on a molecular level at a high throughput level for environmental metabolomics[46]. All samples were mixed to a 60:40 MeOH: ultrapure H_2O ratio and diluted to 1mg L^{-1} carbon at pH 2 using HCl. Prior to injection, a NaTFA tuning mix was used to externally calibrate and internally calibrate sample using three lock masses (i.e. 248.9603, 656.8848 and 928.8344 *m/z*). DOM samples were analyzed in negative ESI mode at a capillary voltage of 4500 V, continuous injection rate of 120µL h^{-1}, and a 0.5 s ion accumulation time to acquire 200 coadded scans in adsorption mode. For each DOM sample, biological duplicates were acquired and only common peaks between replicates were conserved for further analysis.

Peak and formula assignment were conducted using Bruker Compass DataAnalysis (v4.2) with a mass tolerance of ±1ppm and a relative intensity threshold of 0.1%. MeOH, ultrapure H_2O, and media blanks were all subtracted from algal DOM samples prior to further analysis. Coupling FT ICR MS to Cytoscape and MetaNetter2 plugins allowed for the visualization of 105 different transformations encompassing essential amino acids, enzymes, functional groups, and biogenic metal chelating molecules in complex networks[47-49]. Elemental formula and *m/z* values were exported to Cytoscape (Version 3.6.0) equipped with the MetaNetter 2 application to visualize HR-MS *m/z* interactions and transformations within mass spectra[47-49]. User defined chemical interactions (transformations) were then incorporated to allow for the calculation of exact mass differences between two m/z peaks within ±1ppm error.

2.5 Statistical Analyses

A student t-test was applied to evaluate the effect of increasing DOM concentrations on Hg bioavailability. To evaluate the effect of fractionation on Hg uptake, a non-metric multidimensional scaling (NMDS) analysis was conducted using a Euclidian dissimilarity

measure in PAST statistical software v3.0[50]. Bioassay results from all fractionated and unfractionated samples at 1mg C L^{-1} in both aerobic and anaerobic conditions were considered. Clusters were based on significant differences ($p < 0.05$; t-test) and validated by a hierarchical cluster analysis using a Euclidian dissimilarity measure where distinct clusters were defined at a 0.35 cut-off (or at least 65% similarity in composition) (Figure S3). To assess significant differences between bioassay concentration gradients and fractionated material, after testing for normality, a one-way ANOVA was conducted at a confidence interval of 95%. Principal component analyses (PCA) based on correlation were also conducted for F1, F2 and F3 fractions to evaluate how the composition of algal DOM changed after fractionation. Across all three PCAs, 64.3, 62.8 and 68.4% of the total explained variance were explained for F1, F2, and F3, respectively. When addressing compositional differences between Cytoscape derived transformations, a two-way hierarchical cluster analysis and a Spearman's correlation heatmap was conducted using the online tool Heatmapper[51]. Finally, model II regression models were conducted to evaluate the relationship between normalized Hg uptake fluorescence values and the number of Cytoscape transformations. An Akaike information criterion (AIC) test was applied to ensure the strength of the predicted models generated for nonlinear regressions in RStudio (v.1.0153).

Results and Discussion

Effect of DOM Concentration on Mercury Uptake

We first compared the effect of freshly harvested biogenic DOM to the well characterized SRFA. The addition of SRFA (up to 5ppm) decreased Hg uptake by 83.7±1.3% and 65.2±3.7%, under oxic and anoxic conditions, respectively (Figure S4 A-B), in line with previous bioassays[24]. Under both oxic and anoxic conditions, DOM harvested from the Chlorophyta *C. reinhardtii*, *C. vulgaris*, *S. obliquus* and one Euglenozoa species (*E. mutabilis*) decreased Hg uptake by > 90% ($p < 0.001$) at [DOM]=1ppm (Figure 1). Moreover, as little as [DOM] = 0.1 ppm decreased Hg uptake by 50% to 90%, depending on the DOM source. Of the three Chlorophyta tested, *C. reinhardtii* was the least effective at reducing Hg bioavailability at low [DOM] (< 0.5 ppm; Figure 1 B, G). These results are in stark contrast with those obtained using DOM from *E. gracillis*. Although an inhibitory effect was observed, it was to a fewer extent than what was observed for other algae. In this case, the inhibitory effect on Hg bioavailability ranged from 48 to 68% under both aerobic and

anaerobic conditions, respectively (Figure 1 E, J). We speculate that these differences in Hg uptake may stem from different strategies that algae have to cope with toxic metals. Indeed, Chlorophyta and *E. mutabilis* rely on exopolysaccharides (EPS) to limit interactions between the cell and toxic metals[52-54] and such properties have been used for bioremediation purposes in the past[55]. On the other hand, *E. gracilis* has been shown to internalize and reduce Hg^{II} to Hg^{0} [56]; this strategy may have alleviated the need for *E. gracilis* cells to rely on EPS production as a means to protect themselves against toxic metals.

Clearly, the ability of the exudates produced by these diverse phototrophs to affect Hg uptake is species dependent. All species used here were grown autotrophically prior to harvesting their DOM, but some of the organisms are capable of heterotrophic growth (e.g., *C. reinhardtii*, *E. mutabilis* and *E. gracilis*). Although we did not test for the role of carbon metabolism (autotrophy vs. heterotrophy) on the nature of the DOM produced; this is something that should be the focus of further investigations.

Effect of DOM size fractions on Hg uptake

The complex and heterogenous nature of DOM makes it subject to compositional changes depending on environmental conditions[42]. The process of fractionating SRFA resulted in more bioavailable Hg relative to the unfractionated material under both aerobic and anaerobic conditions (Figure S4 C, D). NMDS analysis with Euclidian dissimilarity measure was used to tease apart how AF4 fractionation affected microbial Hg uptake relative to unfractionated algal DOM normalized to 1 $mg{\cdot}C{\cdot}L^{-1}$ (Figure 2; Figure S5). Using this approach, three significant clusters were observed. The first cluster (Figure 2 A) includes size fractions leading to a decrease in Hg uptake (73%) comparable to unfractionated material ($p > 0.05$); these fractions included most large size fractions (F3) from Chlorophyta species and *E. mutabilis*. The second cluster (Figure 2 B) includes mainly F1 and F2 fractions of Chlorophyta. The third cluster includes *E. gracilis* and *S. obliquus* DOM fractions shown to enhance Hg uptake (50.1% for all *E. gracilis* fractions and 25.4% for *S. obliquus* fractions) (Figure 2 C) ($p < 0.05$). *E. mutabilis* DOM led to minimal changes to Hg uptake after fractionation, as all treatments regardless of fractionation or presence of oxygen led to an inhibitory effect on Hg uptake (first cluster; Figure 2 A).

While 1 $mg{\cdot}C{\cdot}L^{-1}$ of unfractionated DOM from all algae significantly ($p < 0.05$) inhibited Hg bioavailability, the process of fractionation led to an overall increase in Hg uptake in all algae

tested, except for *E. mutabilis.* From a biological perspective, unfractionated DOM can act as a dense physical barrier surrounding the bacterial cell walls, and that can sequester Hg[57]. On the other hand, the process of fractionation can lead to increased interactions between metals and the cell wall, which has been shown to enhance toxicity[58]. This is likely due to fractionation leading to exposure of heteroatoms that can participate in metal binding and to a more fluid continuum of molecules surrounding the bacteria. The presence of this continuum may facilitate Hg access to the cell wall and possibly its uptake.

Algal Dissolved Organic Matter Composition

The transformational differences in algal DOM composition determined via Cytoscape network analysis were evaluated using a Spearman's correlation heatmap and a two-way cluster analysis[47, 49] (Figure S6). Three distinct clusters were found along the horizontal axis of the heatmap suggesting similarities in DOM composition based on algal taxa. Specifically, the first cluster (Figure S6 A) is composed of all euglenoid bulk and fractions, except for *E. mutabilis* F3. The second cluster (Figure S6 B) is mainly composed of chlorophyte F1 and F2 fractions, whereas the final cluster (Figure S6 C) consisted of chlorophyte unfractionated DOM and higher molecular weight fractions (F2-F3). Euglenoid DOM was distinct from chlorophyte DOM with significantly greater proportions of polyamine, cytosine, glutamine, serine, and lysine transformations ($p < 0.05$; Figure S6 A). Transformations indicative of glutamine isomers were the most abundant, and especially expressed in *E. gracilis* DOM. The F1-F2 fractions of *E. mutabilis* were comparable to *E. gracilis* fractions; however, *E. mutabilis* fractions were comprised of a greater number of ketol and glyoxylate transformations. Hydrogenation transformations suggestive of highly unsaturated, aliphatic material minimal in double bonds were also abundant in euglenoid DOM.

Although intrinsic differences in algal DOM exist between taxa, the process of fractionation also led to compositional differences within each DOM fraction. Three PCAs were generated for transformations found across F1-F3 (Figure S7 A-C) to reveal how transformations were distributed across AF4 fractions. Euglenoid and chlorophyte DOM were found in two distinct regions of the PCA: positive PC1 and PC2 values for euglenoids and positive PC1 and negative PC2 for chlorophytes in all AF4 fractions. The proximity of the algal vectors was reduced within each algal class as molecular weight increased, suggesting greater similarity in DOM composition within euglenoid and chlorophyte algae in higher molecular weight fractions than smaller size

fractions. Specifically, the F1 fraction of *E. gracilis* was influenced by acetylation (-H) and glutamine transformations and the F1 fraction of *E. mutabilis* comprised condensation/dehydration, lysine and polyamine transformations. *S. obliquus* had contributions from glycine, secondary amines and ethyl transformations and *C. reinhardtii* was abundant in many potential Hg chelating transformations such as cysteine, or ketol. Tertiary amines, C_2H and isoprene transformations were found in *C. vulgaris* F1. *C. vulgaris* and *C. reinhardtii* F2 samples were more similar where hydroxylation, and pyrophosphate can be found in *C. vulgaris* F2 and secondary amines, isoprene and glyoxylate transformations in *C. reinhardtii. S. obliquus* and *E. gracilis* DOM were found to contain amino acids, energy rich trisaccharides, and sugar isomers, that can be favorable sources of energy for bacteria. Finally, all chlorophytes F3 samples were impacted by ketol transformations providing Hg with an electronegative binding site that may account for the overall reduction in Hg uptake across all chlorophyte F3 samples. *E. mutabilis* F3 DOM was mainly influenced by C_2H_2 addition, suggesting homologous DOM, whereas glutamine and glyoxylate transformations remained abundant in *E. gracilis* F3 DOM. Overall, the process of fractionation led to variable proportions of DOM compounds within each fraction, with more variability in DOM composition at lower molecular weights fractions and less variability at higher DOM fractions.

Relationship between Microbial Hg uptake and Algal DOM Composition

To identify which biogenic compounds were most likely altering Hg uptake, spectral networks were used to visualize molecular transformations abundant in euglenoid DOM against normalized aerobic and anaerobic Hg uptake data (Figure 3). Significant positive relationships were found with aerobic Hg uptake for glutamine and serine, and with anaerobic Hg uptake for cytosine, glutamine and polyamine transformations. Given the importance of sulfur functional groups on Hg speciation[59-60], three sulfur containing biogenic isomers including cysteine, methionine and glutathione were identified; however, they were found at greater proportions in Chlorophyta DOM rather than Euglenoid DOM (Figure S6).

Amino acids such as glutamine (Figure 3 A, E; AIC=-2.02, and 1.17 respectively) or serine (Figure 3 B; AIC=-3.49) are essential nutrients for microbial biosynthetic pathways[61-63] being important primary amide donor during the biosynthesis of nucleotides[64-65]. Cytosine (Figure 3 C; AIC= 4.87) is one of the essential nucleotides involved in the formation of DNA and plays a role

in cytidine triphosphate (CTP) formation, an important metabolic cofactor. Soft metals such as Hg and silver (Ag) have been shown to form metal complexes with cytosine and thymine[66-67]. It is possible that binding of Hg to these amine compounds facilitates its accidental transport inside the cell[62, 65]. That being said, we cannot rule out the possibility that these compounds only facilitate the transfer of Hg from solution, through the diffusion boundary layer, to yet unidentified transport sites.

Carboxylic (COOH) transformations were exponentially and negatively correlated with anaerobic Hg uptake (R^2=0.57, p=0.001, AIC=-1.85 Figure 3D). An increase in COOH transformations in DOM yielded an exponential decrease in Hg uptake irrespective of algal or euglenoid taxa (data not shown). Euglenoid DOM yielded the lowest proportion of COOH transformation (0.41-0.80%) whereas Chlorophytes DOM ranged from 0.69-4.34%. Carboxylic acid functional groups are usually associated with higher molecular weight DOM fractions and have a strong affinity for divalent Hg resulting in complexes that are unlikely to pass through biological membranes[69]. These functional group have been identified in *C. vulgaris* and *C. reinhardtii* EPS as responsible for rapidly removing Hg from solution[70-71], further supporting the binding and scavenging role of larger, less bioavailable, multidentate DOM complexes[58-60].

Polyamine transformations were positively related to anaerobic Hg uptake (R^2=0.60, p = 0.001; AIC=-4.92 Figure 3F), with both euglenoid species containing the highest proportion of polyamine transformations, with the strongest influence from *E. gracilis*. The high degree of affinity for Hg to polyamines, the multitude of microbial uptake systems for polyamines[72-75] and the fact that these systems have been reported to facilitate cation transport[76], suggest that polyamine transport represents an underappreciated uptake pathway for Hg. Indeed, in addition from being part of biogenic algal DOM, polyamine compounds such as cadaverine and putrescine are typically produced during the anaerobic fermentative breakdown of amino acids from dead organisms possibly offering a novel route for Hg uptake in anoxic soils and sediments.

Although we observed enhanced Hg uptake in the presence of discrete DOM size fraction when compared to bulk DOM, we did not observe an enhancement of uptake when compared to no DOM controls. This data highlights a very important emergent property of DOM related to how different biomolecules that are comprising the complex DOM pool, interact to affect metal uptake. To the best of our knowledge, the role of such emergent properties of DOM on Hg

bioavailability remains poorly understood. The process of DOM fractionation led to more variable DOM in lower molecular weight fractions whereas similar DOM compositions were observed at higher molecular weight fractions within euglenoids and chlorophyta. The presence of ketol transformations conserved in F3 among all chlorophyta sheds light into the limited Hg uptake of F3 in both aerobic and anaerobic conditions as most Hg may be complexed to the abundant oxygen heteroatoms present in large molecules.

Environmental Implications

Using a multi-pronged approach, we show that DOM from diverse primary producers differentially affect microbial Hg uptake. We propose that amino acids and polyamine biomolecules present in algal DOM are potentially underappreciated ligands involved in enhanced microbial Hg uptake. Our data fits in a broader context where eutrophication, one of the greatest threats to the health of water bodies worldwide, may contribute to conditions increasing Hg bioavailability while also creating conditions optimal for mercury methylation[77]. While unfractionated bulk mixtures of chlorophyte DOM inhibit bacterial Hg uptake, processes leading to fractionation of algal DOM, such as photo or microbial degradation, may trigger periods of increased microbial Hg uptake. Increasing anthropogenic nutrient loading combined with a warming climate stimulate primary production and increase concentrations of autochthonous DOM[78]. One extreme consequence of a stimulation of primary production is eutrophication that causes ecosystem degradation and anoxia. Eutrophication also often leads to shifts in primary producer community structure[79]. Euglenoids and other mixotrophic algae thrive in water or in sediments of eutrophic and hypertrophic aquatic ecosystems[34], suggesting that their increasing abundance under warming conditions may alter Hg bioavailability. Additional work is required to determine the environmental drivers of phytoplankton assemblage in a warming climate and how such drivers will affect primary producer dynamics potentially releasing biogenic compounds controlling the fate of Hg.

Acknowledgements

We thank the members of the Guéguen and Poulain labs for their discussions and insights when preparing this manuscript. We would also like to thank Antoine Perroud for his assistance with DOC analyses, Dr. Chad Cuss for his assistance with field flow fractionation and Dr. Naomi Stock for her help with high resolution mass spectrometry. Special thanks to the Editor and two anonymous reviewers for their insights and feedback to strengthen the manuscript. This study was funded by the Canada Research Chairs program (CG), the Natural Sciences and Engineering Research Council of Canada (AJP, CG, VM), an Early Researcher Award from the Province of Ontario (AJP) and the Canadian Foundation for Innovation (AJP). Funding was also provided by the W. Garfield Weston Doctoral Award for Northern Research (VM).

References

1. Pirrone, N.; Cinnirella, S.; Feng, X.; Finkelman, R. B.; Friedli, H. R.; Leaner, J.; Mukherjee, A. B.; Stracher, G. B.; Streets, D. G.; Telmer, K. Global mercury emission to the atmosphere from anthropogenic and natural sources. *Atmos. Chem. Phys.* **2010**, *10*, 5951-5964; DOI 10.5194/acp-10-5951-2010.

2. Streets D. G.; Zhang Q; Wu Y. Projections of global mercury emissions in 2050. *Environ. Sci. Technol.* **2009**, *43*, 82983–2988; DOI 10.1021/es802474j.

3. Driscoll, C. T.; Mason, R. P; Chan, H. M.; Jacob, D. J.; Pirrone, N. Mercury as a global pollutant: Sources, Pathways and Effects. *Environ. Sci. Technol.* **2013**, *47*, 4967-4983; DOI 10.1021/es305071v.

4. Hintelmann, H. Organomercurials. Their formation and pathways in the environment. *Met. Ions Life Sci.* **2010**, *7*, 365-401; DOI 10.1039/BK9781847551771-00365.

5. Lehnherr, I.; St. Louis, V.; Hintelmann, H.; Kirk, J. L. Methylation of inorganic mercury in polar marine waters. *Nat. Geosci.* **2011**, *4*, 298-302; DOI 10.1038/ngeo1134.

6. Soerensen A. L.; Jacob, D. J.; Schartup, A. T.; Fisher, J. A.; Lehnherr, I.; St. Louis, V.; Heimburger, L. E.; Sonke, J. E.; Krabbenhoft, D. P.; Sunderland, E.M. A mass budget for mercury and methylmercury in the Arctic Ocean. *Glob. Biogeochem. Cycles.* **2016**, *30* (4), 560-575; DOI 10.1002/2015GB005280.

7. Heimbürger L. E.; Sonke, J.; Cossa, D.; Point, D.; Lagane, C.; Laffont, L.; Galfond, B. T.; Nicolaus, M.; Rabe, B.; van der Loeff, M. R. Shallow methylmercury production in the marginal sea ice zone of the central Arctic Ocean. *Sci. Rep.* **2015**, *5* (10318), 1-6; DOI 10.1038/srep10318.

8. Gionfriddo. C. M.; Tate, M. T.; Wick, R. R.; Schulta, M.B.; Zemla, A.; Thelen, M. P.; Schofield, R.; Krabbenhoft, D. P.; Holt, K. E.; Moreau, J. W. Microbial mercury methylation in Antarctic sea ice. *Nat. Microbiol.* **2016**, *1* (10), 16127; DOI 10.1038/nmicrobiol.2016.127.

9. Dranguet, P.; Le Faucheur, S.; Slaveykova, V. I., Mercury bioavailability, transformations, and effects on freshwater biofilms. *Environ. Toxicol. Chem.* **2017**, *36*, (12), 3194-3205; DOI: 10.1002/etc.3934.

10. Olsen, T. A.; Brandt, C. C.; Brooks, S. C. Periphyton biofilms influence net methylmercury production in an industrially contaminated system. *Environ. Sci. Technol*. **2016**, *50*, 10843-10850; DOI 10.1021/acs.est.6b01538.

11. Leclerc, M.; Planas, D.; Amyot, M. Relationship between extracellular low molecular weight thiols and mercury species in natural lake periphytic biofilms. *Environ. Sci. Technol.* **2015**, *49*, 7709-7716; DOI: 10.1021/es505952x.

12. Parks, J. M.; Johs, A.; Podar, M.; Bridou, R.; Hurt, R. A; Smith, S.D.; Tomanicek, S.J.; Qian, Y.; Brown, S. D.; Brandt, C. C.; Palumbo, A. V.; Smith, J. C.; Wall, J. D.; Elias, D. A.; Liang, L. The genetic basis for bacterial mercury methylation. *Science* **2013,** *339*, 1332-1335; DOI 10.1126/science.1230667.

13. Lázaro, W. L.; Guimarães, J. R. D.; Ignácio, A. R.; Da Silva, C. J.; Díez, S., Cyanobacteria enhance methylmercury production: a hypothesis tested in the periphyton of two lakes in the Pantanal floodplain, Brazil. *Sci. Total Environ.* **2013,** *456*, 231-238. DOI 10.1016/j.scitotenv.2013.03.022.

14. Lázaro, W. L.; Díez, S.; da Silva, C. J.; Ignácio, Á. R. A.; Guimarães, J. R. D. Seasonal changes in peryphytic microbial metabolism determining mercury methylation in a tropical wetland. *Sci. Total Environ***. 2018,** *627*, 1345-1352; DOI 10.1016/j.scitotenv.2018.01.186.

15. Gentès, S.; Taupiac, J.; Colin, Y.; André, J. M.; Guyoneaud, R. Bacterial periphytic communities related to mercury methylation within aquatic plant roots from a temperate freshwater lake (South-Western France). *Environ. Sci. Poll. Res.* **2017,** *24* (23), 19223-19233; DOI 10.1007/s11356-017-9597-x.

16. Franco, M. W.; Mendes, L. A.; Windmoller, C. C.; Moura, K. A. F.; Olivera, L. A. G.; Barbosa, F.A. R. Mercury methylation capacity and removal of Hg species from aqueous medium by cyanobacteria. *Water Air Soil Pollut.* **2018**, *229* (127), 1-12; DOI 10.1007/s11270-018-3782-5.

17. Baines, S. B.; Pace, M. L. The production of dissolved organic matter by phytoplankton and its importance to bacteria: Patterns across marine and freshwater systems. *Limnol. Oceanogr.* **1991**, *36*, 1078-1090; DOI 10.4319/lo.1991.36.6.1078.

18. Christensen, G. A.; Somenahally, A. C.; Moberly, J. G.; Miller, C. M.; King, A. J; Gilmour, C. C.; Brown, S. D.; Podar, M.; Brandt, C. C.; Brooks, S. C.; Palumbo, A. V.; Wall, J. D.; Elias, D. A. Carbon amendments alter microbial community structure and net methylmercury potential in sediments. *Appl. Environ. Microbiol.* **2017**, *84* (3), 1-14; DOI 10.1128/AEM.01049-17.

19. Graham, E. B.; Gabor, R. S.; Schooler, S.; McKnight, D. M.; Nemergut, D.R.; Knelman, J. E. Oligotrophic wetland sediments susceptible to shifts in microbiomes and mercury cycling with dissolved organic matter addition. *PeerJ.* **2018**, *6*, (e4575):1-26; DOI 10.7717/peerj.4575.

20. Celo, V.; Lean, D. R. S.; Scott, S. L. Abiotic methylation of mercury in the aquatic environment. *Sci. Tot. Environ.* **2006**, *368* (1), 126-137; DOI 10.1016/j.scitotenv.2005.09.043.

21. Hsu-Kim, H.; Kucharzyk, K. H.; Zhang, T.; Deshusses, M. A. Mechanisms regulating mercury bioavailability for methylating microorganisms in the aquatic environment: a critical

review. *Environ. Sci. Technol.* **2013**, *47*(6): 2441-2456; DOI: 10.1021/es304370g.

22. Liu, G., Cai, Y., & O'Driscoll, N. *Environmental chemistry and toxicology of mercury*. John Wiley & Sons, 2011.

23. Moreau, J. W.; Gionfriddo, C. M.; Krabbenhoft, D. P.; Ogorek, J. M; DeWild, J. F.; Aiken, G. R.; Roden, E. E. The effect of natural organic matter on mercury methylation by *Desulfobulbus propionicus* 1pr3. *Front. Microbiol.* **2015**, *6* (1389), 1-15; DOI 10.3389/fmicb.2015.01389.

24. Chiasson-Gould S. A.; Blais, J. M.; Poulain, A. J. Dissolved organic matter kinetically controls mercury bioavailability to bacteria. *Environ. Sci. Technol.* **2014**, *48*, 3153-3161; DOI 10.1021/es4038484.

25. Graham, A. M.; Bullock, A. L.; Maizel, A. C.; Elias, D. A.; Gilmour, C. C. Detailed assessment of the kinetic of Hg-cell association, Hg methylation, and methylmercury degradation in several *Desulfovibrio* species. *Appl. Environ. Microbiol.* **2012**, *78* (20), 7337-7346; DOI 10.1128/AEM.01792-12.

26. Ortega, S. H.; Catalan, N.; Bjorn, E.; Grontoft, H.; Hilmarsson, T. G.; Bertilsson, S.; Wu, P.; Bishop, K.; Levanoni, O.; Bravo, A.G. High methylmercury formation in ponds fuelled by fresh humic and algal derived organic matter. *Limnol. Oceanogr.* **2018**, *63*, 544-553; DOI 10.1002/lno.10722.

27. Bravo, A. G; Bouchet, S.; Tolu, J.; Bjorn, E.; Mateos-Rivera, A.; Bertilsson, S. Molecular composition of organic matter controls methylmercury formation in boreal lakes. *Nat. Commun.* **2017,** *8*, 1-9; DOI 10.1038/ncomms14255.

28. Graham, A. M.; Aiken, G. R.; Gilmour, C. C. Effect of Dissolved Organic Matter Source and Character on Microbial Hg Methylation in Hg−S−DOM Solutions. *Environ Sci Technol*. **2013,** *47*, 5746-5754; DOI:10.1021/es400414a.

29. Dieguez, M. C.; Queimalinos, C. P.; Guevara, S. R.; DiPasquale, M. M.; Cardenas, C. S.; Arribere, M. A. Influence of dissolved organic matter character on mercury incorporation by planktonic organisms: An experimental study using oligotrophic water from Patagonian lakes. *J. Environ. Sci.* **2013**, *25*, 1980-1991; DOI 10.1016/S1001-0742(12)60281-2.

30. Toming, K.; Tuvikene, L.; Vilbaste, S.; Agasild, H.; Vikk, M.; Kisand, A.; Feldmann, T.; Martma, T.; Jones, R. I.; Noges, T. Contributions of autochthonous and allochthonous sources to dissolved organic matter in a large shallow, eutrophic lake with a highly calcareous catchment. *Limnol. Oceanogr.* **2013**, *58*(4), 1259-1270; DOI:10.4319/lo.2013.58.4.1259.

31. Huertas, E.; Rouco, M.; Lopez-Rodas, V.; Costas, E. Warming will affect phytoplankton differently: evidence through a mechanistic approach. *Proc. R. Soc. B.* **2011**, *278* (1724),

3534-3543; DOI 10.1098/rspb.2011.0160.

32. Bopp, L.; Aumont, O.; Cadule, P.; Alvain, S.; Gehlen, M. Response of diatoms distribution to global warming and potential implications: A global model study. *Geophys. Res. Lett.* **2005,** *32* (19), 1-4; DOI 10.1029/2005GL023653.

33. Paerl, H.W.; Gardner, W.S; Havens, K.E; Joyner, A.R; McCarthy, M.J; Newell, S.E; Qin, B.; Scott, T. Mitigating cyanobacterial harmful algal blooms in aquatic ecosystems impacted by climate change and anthropogenic nutrients. *Harmful Algae* **2016**, *54*, 213-222; DOI 10.1016/j.hal.2015.09.009.

34. Winder, M.; Sommer, U. Phytoplankton response to a changing climate. *Hydrobiol.* **2012**, *698*, 5-16; DOI 10.1007/s10750-012-1149-2.

35. Benoit, J. M.; Mason, R. P.; Glimour, C.C.; Aiken, G. R. Constant for mercury binding by dissolved organic matter isolates from the Florida Everglades. *Geochim. Cosmochim. Acta.* **2001**, *65*, 4445-4451; DOI 10.1016/S0016-7037(01)00742-6.

36. Miller, C. L.; Mason, R. P.; Gilmour, C. C.; Heyes, A. Influence of dissolved organic matter on the complexation of mercury under sulfidic conditions. *Environ. Toxicol. Chem.* **2007**, *26* (4), 624-633; DOI 1897/06-375R.1.

37. Dasgupta, S.; Fang, J.; Brake, S. S.; Hasiotis, S. T.; Zhang, L. Biosynthesis of sterols and wax esters by *Euglena* of acid mine drainage biofilms: Implications for eukaryotic evolution and the early Earth. *Chem. Geol.* **2012**, *306-307*, 139-145; DOI 10.1016/j.chemgeo.2012.03.003.

38. Khohn-Molt, I.; Wemheuer, B.; Alawi, M.; Poehlein, A.; Gullert, S.; Schmeisser, C.; Pommerening-Roser, A.; Grundhoff, A.; Daniel, R.; Hanelt, D.; Streit, W. R. Metagenome survey of multispecies and alga-associated biofilm revealed key elements of bacterial-algal interactions in photobioreactors. *Appl. Environ. Microbiol.* **2013**, *79* (20), 6196-6206; DOI 10.1128/AEM.01641-13

39. Mangal, V.; Guéguen, C. Examining concentrations and molecular weights of thiols in microorganism cultures and in Churchill River (Manitoba) using a fluorescent-labeling method coupled to asymmetrical flow field-flow fractionation. *Anal. Bioanal. Chem.* **2015**, *407* (15), 4305-4313; DOI 10.1007/s00216-015-8599-0.

40. Guéguen, C.; Cuss, C. Characterization of aquatic dissolved organic matter by asymmetrical flow field-flow fractionation coupled to UV-Visible diode array and excitation emission matrix fluorescence. *J. Chromatogr. A.* **2011**, *1218* (27), 4188-4198; DOI 10.1016/j.chroma.2010.12.038.

41. Reszat, T. N.; Hendry, J. M. Characterizing dissolved organic carbon using asymmetrical flow field flow fractionation with on-line UV and DOC detection. *Anal. Chem.* **2005**, *77*, 4194-4200; DOI 10.1021/ac048295c.

42. Kujawinski, E. B; Freitas, M. A.; Zhang, X.; Hatcher, P. G.; Green-Church, K. B.; Jones, B, R. The application of electrospray ionization mass spectrometry (ESI MS) to the structural characterization of natural organic matter. *Org. Geochem.* **2002**, *33*, 171-180; DOI 10.1016/S0146-6380(01)00149-8.

43. Stenzler, B.; Hinz, A.; Ruuskanen, M.; Poulain, A. J. Ionic strength differentially affects the bioavailability of neutral and negatively charged inorganic Hg complexes. *Environ. Sci. Technol.* **2017,** *51*, 9653-9662; DOI 10.1021/acs.est.7b01414.

44. Winters, C.; Guéguen, C.; Noble, A. Equilibrium and kinetic studies of Cu (II) and Ni (II) sorption on living *Euglena gracilis. J. Appl. Phycol.* **2017**, *29* (3), 1391-1398; DOI 10.1007/s10811-016-1040-z

45. Drepper, T.; Eggert, T.; Circolone, F.; Heck, A.; Krauss, U.; Guterl, J. K.; Wendorff, M.; Losi, A.; Gartner, W.; Jaeger, K. E. Reporter proteins for in vivo fluorescence without oxygen. *Nat. Biotechnol.* **2007**, *4*, 443-435. DOI:10.1038/nbt1293

46. Viant, M. R.; Sommer, U. Mass spectrometry based environmental metabolomics: a primer and review. *Metabolomics.* **2013**, *9*, 144-1568; DOI 10.1007/s11306-012-0412-x.

47. Longnecker, K.; Kujawinski, E. B. Using network analysis to discern compositional patterns in ultrahigh resolution mass spectrometry data of dissolved organic matter. *Rapid Commun. Mass Spectrom.* **2016**, *30*, 2388-2394; DOI 10.1002/rcm.7719.

48. Burgess, K. E. V.; Borutzki, Y.; Rankin, N.; Jourdan, F. MetaNetter 2: A Cytoscape plugin for ab initio network analysis and metabolite feature classification. *J. Chromatogr. B.* **2017**, *1071*, 68-74; DOI 10.1016/j.jchromb.2017.08.015.

49. Mangal, V.; Shi, Y. X.; Guéguen, C. Compositional changes and molecular transformations of dissolved organic matter during the arctic spring floods in the lower Churchill watershed (Northern Manitoba, Canada). **2017,** *136* (2), 151-165; DOI 10.1007/s10533-017-0388-8.

50. Hammer, O.; Harper, D. A. T.; Ryan, P. D. Paleontological statistics software package for education and data analysis. *Palaeontologia Electronica.* **2011**, *4* (1), 1-9; http://palaeo-electronica.org/2001_1/past/issue1_01.htm.

51. Babicki, S.; Arndt, D.; Marcu, A.; Liang, Y; Grant, J.R; Maciejewski, A; Wishart, D.S. Heatmapper: web-enabled heat mapping for all. *Nucleic Acids Res.* **2016**, *8*, 147-153; DOI 10.1093/nar/gkw419.

52. Zhou, K.; Hu, Y.; Yang, K.; Lin. The role of exopolymeric substances in the bioaccumulation and toxicity of Ag nanoparticles to algae. *Sci. Rep.* **2016**, *6*, 32998; DOI: 10.1038/srep32998.

53. Decho, A.; W; Gutierrez, T. Microbial Extracellular Polymeric Substances (EPSs) in Ocean Systems. *Front. Microbiol.* **2017**, *8*, 922; DOI 10.3389/fmicb.2017.00922.

54. Gupta, P.; Diwan, B. Bacterial Exopolysaccharide mediated heavy metal removal: a review on biosynthesis, mechanism and remediation strategies. *Biotechnol. Rep.* **2017,** *13*, 58-71; DOI 10.1016/j.btre.2016.12.006.

55. Zeraatkar, A. K.; Ahmadzadeh, H.; Talebi, A. F.; Moheimani, N. R.; McHenry, M. P. Potential use of algae for heavy metal bioremediation, a critical review. *J. Environ. Manage.* **2016,** *181*, 817-831; DOI:10.1016/j.jenvman.2016.06.059.

56. Devars, S.; Aviles, C.; Cervantes, C.; Moreno-Sanchez, R. Mercury uptake and removal by Euglena gracilis. *Arch. Microbiol.* **2000,** *174*, (3), 175-80; DOI 10.1007/s002030000193.

57. Koukal,;Gueguen, C.; Pardos, M.; Dominik, J. Influence of humic substances on the toxic effects of cadmium and zinc to the green alga Pseudokirchneriella subcapitata. *Chemosphere.* **2003**, *53*, (8), 953−961; DOI:10.1016/S0045-6535(03)00720-3.

58. Smith, K.S.; Balistrieri, L.S.; Todd, A.S. Using biotic ligand models to predict metal toxicity in mineralized systems. *Appl. Geochem.* **2015**, 57, 55-72; DOI:/10.1016/j.apgeochem.2014.07.005.

59. Hesterberg, D.; Chou, J. W.; Hutchinson, K. J.; Sayers, D. E. Bonding of Hg(II) to reduced organic sulfur in humic acid as affected by S/Hg ratio. *Environ. Sci. Technol.* **2001**, *35*(13), 2741-2745. DOI**:** 10.1021/es001960o.

60. Haitzer, M.; Aiken, G. R.; Ryan, J. N. Binding of mercury (II) to dissolved organic matter: The role of the mercury to DOM concentration ratio. *Environ. Sci. Technol.* **2002**, *36*, 3564-3570. DOI 10.1021/es025699i.

61. Weiner J. H.; Heppel, L. A. A binding protein for glutamine and its relation to active transport in *E.Coli. J. Biol. Chem.* **1971**, *246*, 6933-6941.

62. Forchhammer, K. Glutamine signaling in bacteria. *Front. Biosci.* **2007**, *12***,** 358-70; DOI 10.2741/2069.

63. Schaefer, J. K.; Morel, F. M. M. High methylation rates of mercury bound to cysteine by *Geobacter sulfurreducens. Nat. Geosci.* **2009**, *2*, 123-126. DOI: 10.1038/ngeo412

64. Prusiner S, & Stadtman E. R. *The enzymes of glutamine metabolism. Academic Press, Inc, New York, NY* (1973).

65. Tanaka, K. J.; Song, S.; Mason, K.; Pinkett, H. W. Selective substrate uptake: The role of ATP-binding cassette (ABC) transporters in pathogenesis. *BBA- Biomembranes*. **2018**, *1860*, 866-877; DOI 10.1016/j.bbamem.2017.08.011.

66. Ono, A.; Cao, S.; Togashi, H.; Tashiro, M.; Fujimoto, T.; Machinami, T.; Miyake, Y.; Okamoto, I.; Tanaka, Y. Specific interactions between silver(I) ions and cytosine-cytosine pairs in DNA duplexes. *Chem. Commun.* **2008**, *39*, 4825-4827; DOI:10.1039/b808686a.

67. Yamaguchi.; Sebera, J.; Kondo, J.; Komuro, T.; Kawamura, T.; Dairaku, T.; Kondo, Y.; Okamoto, I.; Ono, A.; Burda, J. B.; Kojima, C.; Sychrovsky, V.; Tanaka, Y. The structure of metallo-DNA with consecutive thymine-Hg^{II}-thymine base pairs explains positive entropy for the metallo base pair formation. *Nucl. Acid Res.* **2014**, *42*(6), 4094-4099. DOI: 10.1093/nar/gkt1344.

68. Nies, D. H. Microbial heavy-metal resistance. *Appl. Micro. Biotech.* **1999**, *51* (6), 730-750; DOI 10.1007/s002530051457.

69. Ndu, U.; Mason, R. P.; Zhang, H.; Lin, S.; Visscher, P. T. Effect of inorganic and organic ligands on the bioavailability of methylmercury as determined using a *mer-lux* bioreporter. *Appl. Environ. Microbiol.* **2012**, *78* (20), 7276-7282; DOI 10.1128/AEM.00362-12.

70. Tuzun, I.; Bayramoglu, G.; Yalcin, E.; Basaran, G.; Celik, G.; Arica, M. Y. Equilibrium and kinetic studies on biosorption of Hg(II), Cd(II) and Pb(II) ions onto microalgae Chlamydomonas reinhardtii. *J. of Environ. Manag.* **2005,** *77* (2), 85-92; DOI 10.1016/j.jenvman.2005.01.028.

71. Peng, Y.; Liu, X.; Gong, X.; Li, X.; Liu, Y.; Leng, E.; Zhang, Y. Enhanced Hg(II) Adsorption by Monocarboxylic-Acid-Modified Microalgae Residuals in Simulated and Practical Industrial Wastewater. *Energy & Fuels* **2018,** *32*, (4), 4461-4468.

72. Foti, C.; Giuffre, O.; Lando, G.; Sammartano, S. Interaction of inorganic mercury (II) with polyamines, polycarboxylates and amino acids. *J. Chem. Eng. Data.* **2009**, *54*, 893-903; DOI 10.1021/je800685c.

73. Halvorson, H. Utilization of single L-amino acids as sole source of carbon and nitrogen by bacteria. *Can. J. Microbiol.* **1972**, *18*, 1647-1650.

74. Igarashi, K.; Kashiwaqi, K. Polyamine uptake systems in *Escherichia coli. Res. Microbiol.* **2001**, *152*, 271-278; DOI 10.1016/S0923-2508(01)01198-6.

75. Kurihara, S.; Suzuki, H. Recent advances in bacterial polyamine transport systems. *Polyamines.* **2014**, 171-178; DOI 10.1007/978-4-431-55212-3_14.

76. Pottosin, I.; Shabala, S. Polyamines control of cation transport across plant membranes: implications for ion homeostasis and abiotic stress signaling. *Front. Plant. Sci.* **2014**, *5* (154), 1-16; DOI 10.3389/fpls.2014.00154.

77. Krabbenhoft, D. P.; Sunderland, E.M. Global change and mercury. *Science* **2013**, *341*, 1457-1458. DOI: 10.1126/science.1242838.

78. Heinsalu, A.; Alliksaar, T.; Leeben, A.; Noges, T. Sediment diatom assemblages and composition of pore-water dissolved organic matter reflect recent eutrophication history of Lake Peipsi (Estonia/Russia). *Hydrobiol.* **2007**, *584*, 133-143.

79. Hallegraeff, G.M. Ocean climate change, phytoplankton community responses, and harmful algal blooms: a formidable predictive challenge. *J. Phycol.* **2010**, *46*, 220-235. DOI 10.1111/j.1529-8817.2010.00815.x.

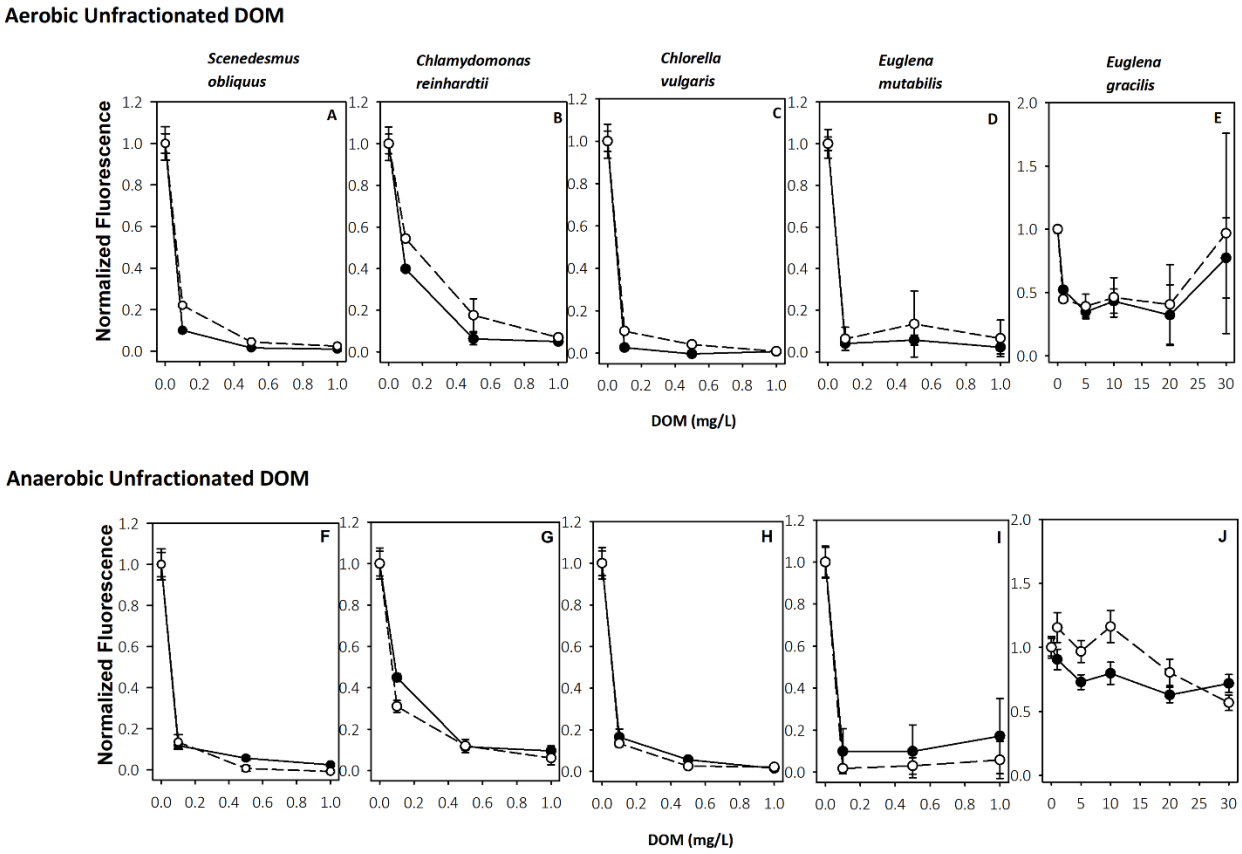

700

701 **Figure #1:** Aerobic (A-E) and anaerobic (F-J) bioassays with increasing DOM concentrations
702 from algal cultures of *S. obliquus* (A, F), *C. reinhardtii* (B, G), *C. vulgaris* (C, H), *E. mutabilis*
703 (D, I) and *E. gracilis* (E, J) where n=3.

704

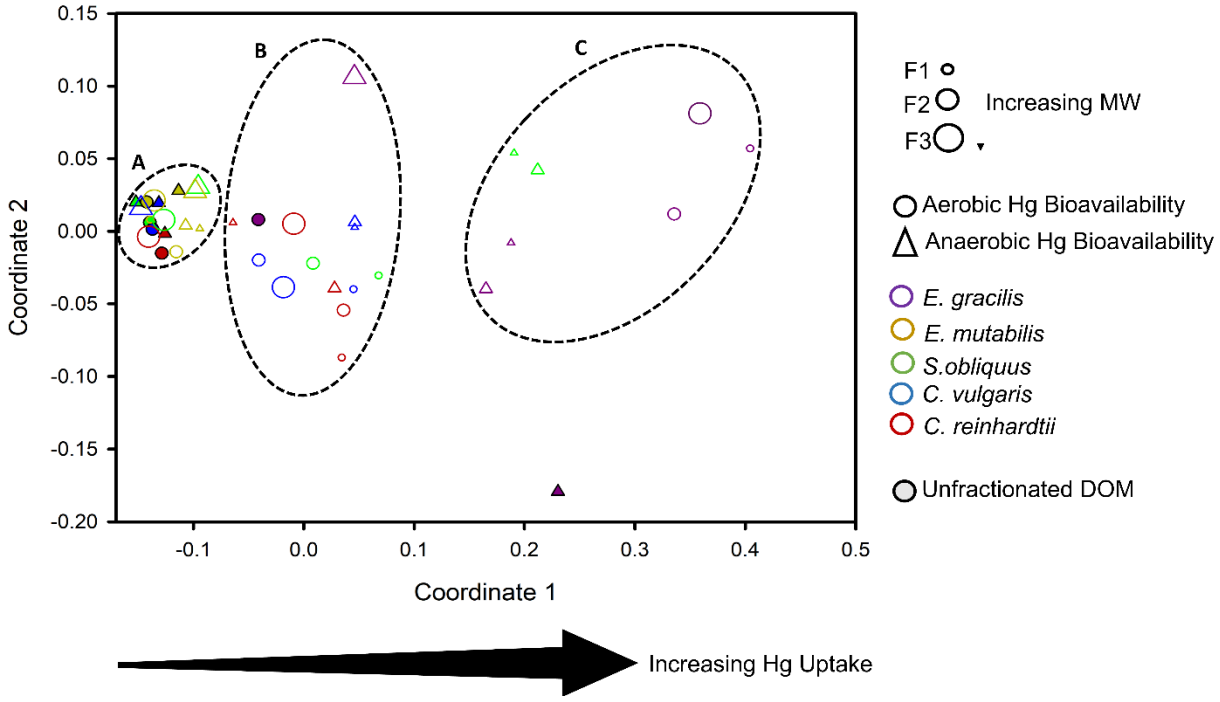

705

706 **Figure #2:** NMDS using a Euclidian measure analysis portraying the effect of algal DOM
707 fractionation and Hg uptake. ○ represent aerobic assays whereas △ represent anaerobic
708 bioassays with the size of each symbol corresponding to the molecular weight fraction with ○
709 =F1, ○ =F2 and ○ =F3. Colours correspond to algal taxa where purple is *E. gracilis*, yellow
710 is *E. mutabilis*, green is *S. obliquus*, blue is *C. vulgaris*, and red is *C. reinhardtii*. Filled symbols
711 outline unfractionated DOM and dashed lines show significant clustering.

712

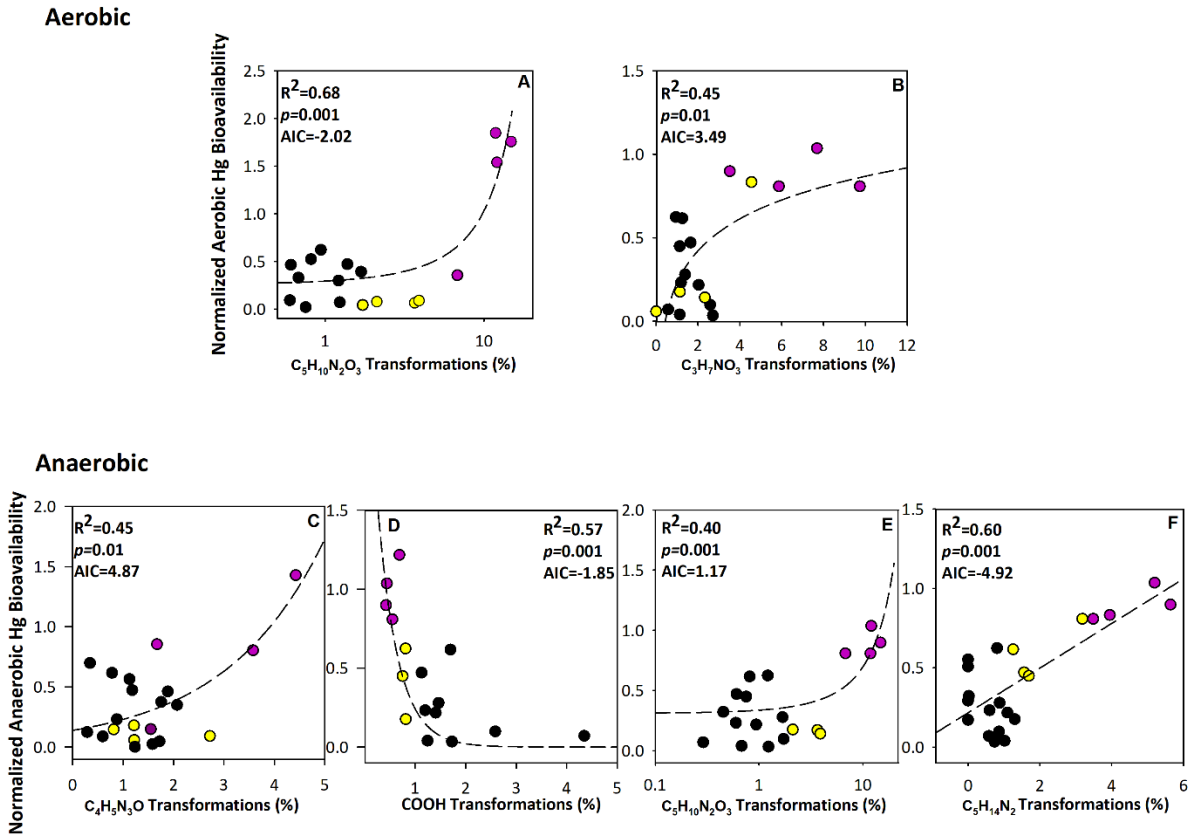

713

714 **Figure #3:** Significant Model II regression models outlining relationships between aerobic Hg
715 uptake and $C_5H_{10}N_2O_3$ (glutamine; A), and $C_3H_7NO_3$ (serine; B) isomers. Anaerobic Hg uptake
716 and biomolecules are also expressed for $C_4H_5N_3O$ (cytosine; C), COOH functional groups (D),
717 $C_5H_{10}N_2O_3$ (glutamine; E) and $C_5H_{14}N_2$ (polyamine; F) isomers. Both Euglenoids are highlighted
718 where yellow corresponds to points corresponding to *E. mutabilis* and purple highlights points
719 influenced by *E. gracilis.*

720